Journal of Molecular Catalysis A: Chemical 426 (2017) 88–96

Contents lists available at ScienceDirect

Journal of Molecular Catalysis A: Chemical

journal homepage: www.elsevier.com/locate/molcata

Preparation of acetates catalyzed by boric acid and/or tungstophosphoric acid-modified zirconia obtained employing polyethylene glycols as pore-forming agents

Lilian Osiglio, Gabriel Sathicq, Luis Pizzio*, Gustavo Romanelli, Mirta Blanco

Centro de Investigación y Desarrollo en Ciencias Aplicadas "Dr. J. J. Ronco" (CINDECA), Departamento de Química, Facultad de Ciencias Exactas, UNLP-CCT La Plata, CONICET, 47 N° 257, 1900 La Plata, Argentina

ARTICLE INFO

Article history:
Received 2 August 2016
Received in revised form 11 October 2016
Accepted 2 November 2016
Available online 4 November 2016

Keywords:
Acetates
Aroma compounds
Boric acid and/or tungstophosphoric acid-modified zirconia
Polyethylene glycols

ABSTRACT

Zirconia modified with boric acid and/or tungstophosphoric acid calcined at 320 °C were prepared, characterized and used as catalysts in the production of acetates from diverse alcohols and phenols. Polyethylene glycol (PEG) of different molecular weight (400, 2000, 6000 Da) were added as low cost pore-forming agents during zirconia synthesis using zirconyl chloride as precursor and ammonium hydroxide as precipitating agent. The zirconias were impregnated with aqueous solutions of boric acid and/or tungstophosphoric acid (TPA). The borated zirconias, zirconias modified with TPA and zirconias doped with both boron and TPA were amorphous mesoporous materials with very strong acid sites, and specific surface areas S_{BET} of around 200, 100, and 150 m^2/g, respectively. The FT-IR spectra of borated zirconias exhibited the bands of boron species, while the zirconias modified with TPA presented the characteristic bands of tungstophosphate anion, and the zirconias doped with both boron and TPA showed a degradation of the TPA anion, confirmed by ^{31}P MAS-NMR. The borated zirconias and the zirconias modified with TPA gave excellent selectivity and yield in the 2-phenylethanol esterification with acetic acid. The use of these materials allows obtaining higher or similar results than those reported in the literature. Zirconias doped with both boron and TPA gave lower values, due to the transformation of the $[PW_{12}O_{40}]^{3-}$ Keggin anion in to the $[P_2W_{21}O_{71}]^{6-}$ and $[PW_{11}O_{39}]^{7-}$ species. The reactivity towards acetylation with acetic acid of different alcohols and phenols using the best catalyst was ordered according to: primary alcohols > secondary alcohols > phenols. The reactivity difference of the alcohols and phenols was correlated with the electronic density on the oxygen atom and steric effects.

1. Introduction

The preparation of organic esters through the esterification reaction between a carboxylic acid and an alcohol is the most studied chemical transformation in organic chemistry, due to the wide application of the esters that may be formed. Esters are useful molecules because of their diverse applications, such as fragrances, flavours, solvents, synthesis intermediates and drug products of interest. Furthermore, the conversion of alcohols and phenols to esters is a significant synthetic transformation that has received considerable attention [1] because it is an efficient method to protect hydroxyl groups in multistep synthetic processes [2,3]. Among the various protecting groups of the hydroxyl function, the acetyl group is the most appropriate in view of its easy introduction and stability in acidic conditions [4,5].

Many esters are flavour and fragrance compounds, which are widely used in food, cosmetic, beverage and pharmaceutical industries. In particular, the 2-phenylethyl acetate has a pleasant rose aroma, and is widely used to add scent or flavour to cosmetics, soaps, foods and drinks, giving the two latter a hint of fruit wine aroma [6].

Nowadays, the demand for esters has notably increased. They have usually been obtained from plants, but some factors make synthetic production essential. Among them, it can be mentioned that the vegetation may suffer the influence of weather or diseases and, in addition, the quantities obtained by extraction from natural sources are small [7].

The reaction involved to obtain esters is usually catalyzed by classical acids. There are many updated procedures though, as reported by Shirini et al. [8], some of the methods show vary-

* Corresponding author.
E-mail addresses: lrpizzio@quimica.unlp.ar, lrpizzio@hotmail.com (L. Pizzio).

http://dx.doi.org/10.1016/j.molcata.2016.11.004
1381-1169/

ing degrees of success and limitations, such as long reaction time, strong reaction conditions, the occurrence of side reactions, as well as low yields of the desired product. Thus, the development of alternative clean procedures for the acetylation reaction is highly needed. In this direction, our research group has experience in the friendly ester synthesis using acetic acid as acetylating agent and an alcohol or phenol with different structures. Two different catalyst families were used: zirconium oxide doped with boron [9] and ammonium metatungstate-modified borated zirconia [10], and in both cases the acetylation was strongly dependent on the alcohol structure.

As is well known, the preparation of new acid solids is an important field in order to replace the traditional acids, bearing in mind the need to achieve clean processes to protect the environment. In this context and due to our experience in the preparation of catalysts based on a special type of compounds, with strong acidic characteristics, such as the heteropolycompounds with Keggin structure [e.g.,11–14], which were tested as catalysts in different reactions [e.g.,15–20], including isoamyl acetate production by esterification [e.g.,21,22], it was decided to add TPA to borated zirconia in order to compare the results with samples prepared without boron addition. Recently, an unsupported mixture of a Keggin heteropolyacid and boric acid in an ionic liquid as solvent was used to obtain 5-hydroxymethylfurfural [23].

Moreover, as diverse pore-forming compounds, such as hydroxyacids or urea [24–26], may be added to improve the textural properties of different oxides, in a previous work glucose and polyethylene glycol of different molecular weight were employed as low cost pore-forming agents, observing that polyethylene glycol may effectively be used to obtain mesoporous zirconia with higher specific surface area and pore size than without its addition [27].

In this context, the aim of the present study was to synthesize 2-phenylethyl acetate, an essential aroma component for the food and cosmetic industries, by Fischer catalyzed esterification between 2-phenylethanol and acetic acid, and then to study the behaviour of different alcohols and phenols in catalyzed acetate production. It is known that acetic acid is a cheap reagent and only forms water as a by-product, so it will be a clean process. Diverse materials based on boric acid and/or tungstophosphoric acid-modified zirconias were used as catalysts, using zirconias prepared with polyethylene glycol of different molecular weight as pore-forming agents. The physicochemical characteristics of the prepared catalysts and the electronic density on the oxygen atoms in the alcohols and phenols were studied in order to correlate them with the reaction results obtained.

2. Experimental

2.1. Sample preparation

Zirconia was prepared employing an aqueous solution of $ZrOCl_2{\cdot}8H_2O$ (Fluka) (0.56 mol Zr/dm^3) as precursor, to which ammonium hydroxide 30% (Merck) was added drop-wise as precipitating agent up to a final pH of 10, under constant stirring. The effect of the addition of 10% (w/w) of polyethylene glycol (PEG) of molecular weights 400, 2000 or 6000 Da as pore-forming agents, which were added during the hydrogel preparation, was studied. The obtained products were aged for 72 h and filtered under vacuum. The precipitates were washed with distilled water to remove PEG and chlorides, up to negative reaction with $AgNO_3$ in the washings. The supports, dried at room temperature (r.t.), were impregnated with H_3BO_3 (Anedra p.a.) aqueous solution of 0.3 mol B/dm^3 concentration, to obtain a boron concentration of 15% (w/w) in the solid, expressed as B_2O_3 with respect to the support. The samples to which PEG400, PEG2000 and PEG6000 were added will be named ZrP4B, ZrP20 B and ZrP60B, respectively. After drying at r.t., the borated zirconias were impregnated with a tungstophosphoric acid (TPA) solution of 0.04 mol W/dm^3 concentration that leads to 15%W (w/w) in the solid, thus obtaining the samples named ZrP4BTPA, ZrP20BTPA and ZrP60BTPA. The boron and tungsten concentration in the samples were chosen taking into account the results published in previous report [9,10]. The solids were dried at r.t. and calcined in N_2 atmosphere for 5 h at 320 °C. Materials with TPA but without boric acid addition calcined at the same temperature (ZrP4TPA, ZrP20TPA, ZrP60TPA samples) were prepared for comparison purposes.

2.2. Sample characterization

The specific surface area, the pore volume and the pore size of the solids were estimated from the adsorption-desorption isotherms of nitrogen at −196 °C, using Micromeritics equipment, model ASAP 2020, and previous degasification at 100 °C for 1 h.

The X-ray diffraction (XRD) patterns were recorded between 5 and 60° 2θ with Philips PW-1732 equipment with a built-in recorder, using Cu Kα radiation, Ni filter, 20 mA and 40 kV in the high tension source, and a scanning rate of 1° per min.

The infrared (FT-IR) spectra were acquired employing Bruker IFS 66 equipment and pellets of the sample in KBr. The measurements were performed in the 400–4000 cm^{-1} range.

For the analysis by ^{31}P MAS–NMR, Bruker MSL-300 equipment with a sample holder of 5 mm diameter and 10 mm in height was employed, using 5 s pulses, a repetition time of 3 s, working at a frequency of 121.496 MHz for ^{31}P at room temperature. The spin rate was 2.1 kHz, and several hundred pulse responses were collected. Phosphoric acid 85% was employed as external reference.

To obtain the micrographs of the solids, scanning electron microscopy (SEM) was employed, using Philips equipment, model 505, at a working potential of 15 kV, supporting the samples on graphite and metallizing with a sputtered gold film. The images were obtained with ADDAII acquisition device, with Soft Imaging System, using magnification between 300 and 5000×.

The materials were potentiometrically titrated in order to estimate their acidity. To this end, 0.05 g of solid was suspended in 45 cm^3 of acetonitrile. The suspension was stirred for 3 h, and then titrated with a 0.025 N solution of *n*-butylamine in acetonitrile. The potential variation was measured with Metrohm 794 Basic Titrino apparatus with a double-junction electrode.

2.3. Catalytic evaluation

2.3.1. General

Chemicals were purchased from Fluka, Merck and Aldrich companies. The yields refer to the isolated pure product. Products were characterized by IR and NMR spectroscopy and mass spectrometry. Proton nuclear magnetic resonance (^{1}H NMR) experiments were recorded on Avance DPX 400, Bruker (400 MHz) spectrophotometer. Carbon nuclear magnetic resonance (^{13}C NMR) was recorded on Avance DPX 400, Bruker (400 MHz) spectrometer with tetramethylsilane (TMS) as the internal standard. All chemical shifts are quoted in parts per million (ppm) relative to TMS using deuterated solvent. Coupling constants (*J*) are given in hertz (Hz). Signal splitting is described as singlets (s), doublets (d), double doublet (dd), triplet (t), quartets (q), and multiplets (m). Gas chromatography coupled with mass spectrophotometer was done on HP 5971 instrument and mass recorded in EI mode. Infrared (IR) spectra were acquired employing Bruker IFS 66 equipment and pellets of the sample in KBr. Absorption maxima are quoted in wavenumbers (cm^{-1}) and only structurally significant peaks are listed.

The electronic density of the oxygen atoms in the alcohols and phenols was determined after optimization of their conforma-

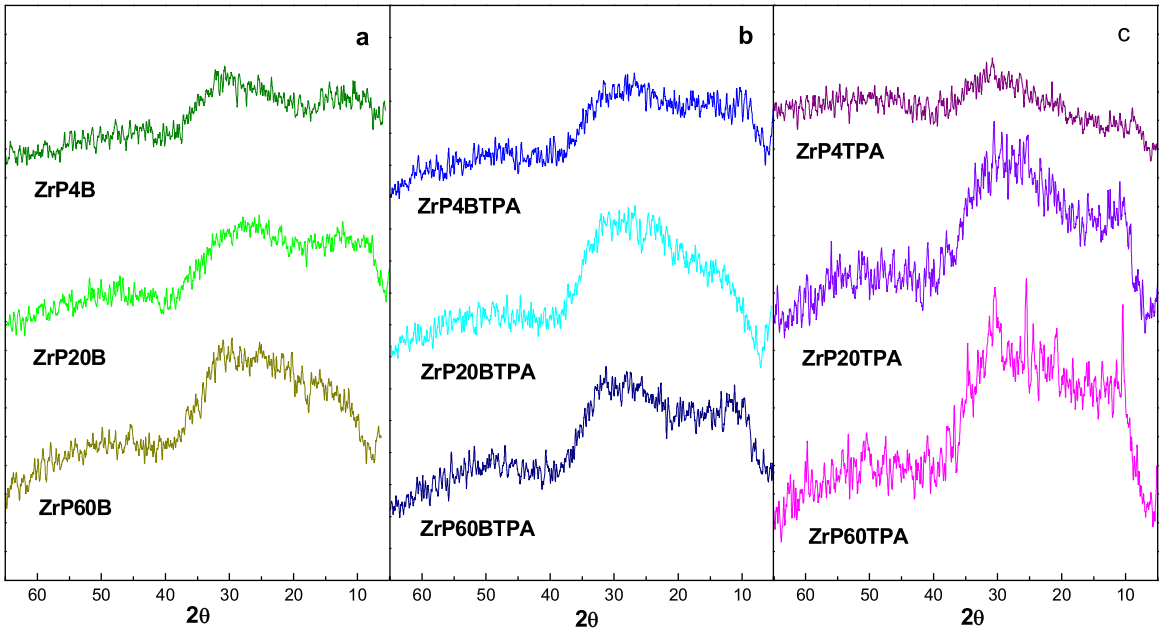

Fig. 1. XRD patterns of the samples obtained using PEG with different molecular weight as pore-forming agents: a) borated zirconias, b) tungstophosphoric acid-modified borated zirconias, c) tungstophosphoric acid-modified zirconias.

tion. The conformation of the compounds was drawn by means of the "model build" modulus available in HyperChem 5.0. Each molecular structure was firstly preoptimized with the Molecular Mechanics Force Field (MM +) procedure, and the resulting geometry was further refined by means of the semi-empirical method PM3 (Parametric Method-3). A gradient norm limit of 0.01 kcal $Å^{-1}$ was chosen.

2.3.2. Catalytic test

In all the reactions, a 25 cm^3 round-bottomed flask, at the reaction temperature and connected with a water jacketed condenser, was used. In a typical experience, the reactor was loaded with a mixture of 1 mmol of 2-phenylethanol (122 mg), 5 mmol of acetic acid (300 mg), 5 cm^3 of toluene and 100 mg of the catalyst. The mixture was stirred at 700 rpm. Samples were withdrawn from the organic phase at different intervals (1, 3, 5, 7, 10 and 14 h). Each sample volume was approximately 10 mm^3 and was diluted with 2 cm^3 of acetonitrile. The concentration of substrates was calculated with the corresponding areas, using a Shimadzu HP2010 gas chromatography instrument (Chromopack CP Sil 8 CB, 30 m × 0.32 mm ID). A similar procedure was followed with the other studied alcohols and phenols.

After 14 h of reaction, the solution was concentrated under vacuum, and the residue was purified by column chromatography employing silica gel as the stationary phase and a mixture of hexane-ethyl acetate as the elution solvent. The reaction products were identified by chromatographic comparison with standard samples. The conversion was expressed as the ratio of moles of products to moles of initial alcohol.

2.3.3. Catalyst reuse

The stability tests were carried out running three consecutive experiments, under the same reaction conditions. After each test, the catalyst was separated from the reaction mixture by simple filtration, washed twice with 2 cm^3 toluene, dried under vacuum at room temperature for 4 h, and then reused.

3. Results and discussion

3.1. Catalyst characterization

The X-ray diffraction patterns of all the prepared solids presented a broad band with maximum placed at 2θ = 30° (Fig. 1), indicating zirconia amorphous nature [28]. The patterns of the samples modified with boron and/or TPA were similar to those of the respective supports, with the absence of crystalline phases. The only exception is the pattern of the ZrP60TPA sample, in which very low signals that may be assigned to TPA are placed at 2θ = 10°, 25° and 35°. Though the pattern of tungstophosphoric acid depended on the hydration degree of the acid, these lines are characteristic of TPA with a low hydration degree. Besides, it must be mentioned that peaks assigned to boric acid or boric oxide were not present in the patterns of the samples. So, it can be inferred that in almost all the samples the boron and TPA species are well dispersed on the surface of the support as a non-crystalline phase, without forming the structure needed to attain a diffraction pattern, or crystallites too small to give diffraction lines are present. In addition, any of the different crystalline phases of zirconia were noticed, although a stabilization effect can be induced by the presence of impurities, as was reported by Yamaguchi [29,30].

The specific surface area (S_{BET}), determined by the Brunauer-Emmett-Teller method, of a zirconia sample obtained without the addition of PEG during the synthesis (Zr sample), were 146 m^2/g. The microporous area (S_{micro}), estimated by the t-plot method was almost negligible (12 m^2/g) and its mean pore size (MPS), estimated by the Barrett-Joyner-Halenda (BJH) method from the desorption branch of the isotherm, was 2.1 nm. In the case of the zirconia samples (ZrP4, ZrP20, and ZrP60) obtained adding PEG during the synthesis, a significantly increment of the MPV values was revealed (3.0–3.1 nm). However, this increment does not depend on the polyethylene glycol molecular weight. On the other hand, the specific surface area S_{BET} remains practically unchanged, slightly increases (~16%) or decrease (~20%) when PEG 400, 2000 or 6000, respectively, were used as pore forming agent. According to the S_{micro} values, less than 10% of specific surface area is due to the presence of microporous. So, these results indicate that the use of

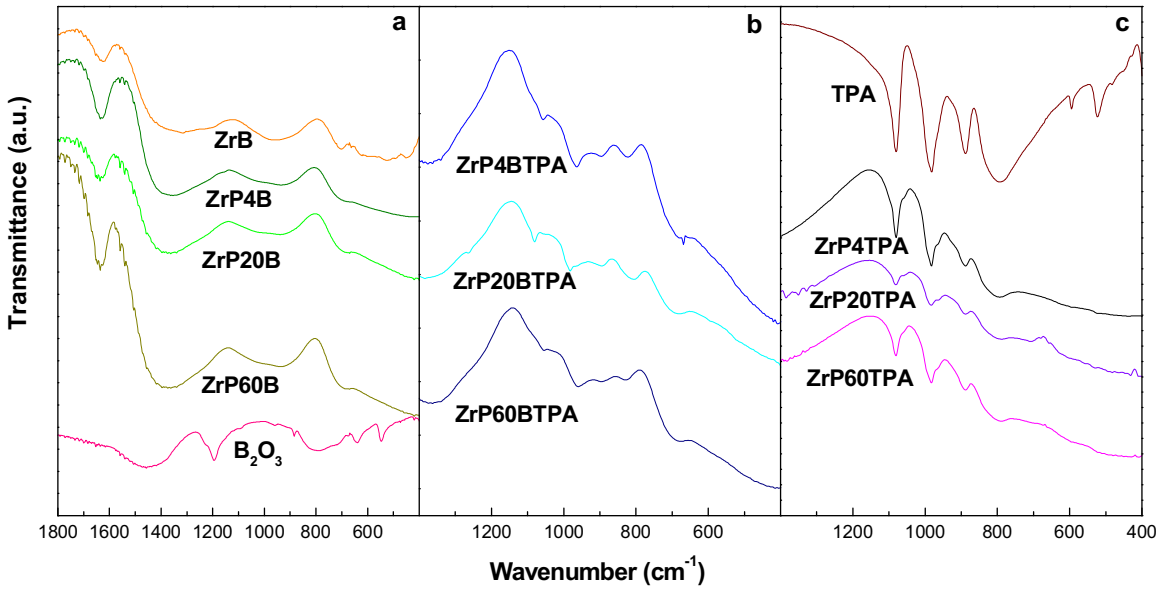

Fig. 2. FT-IR spectra of the samples obtained using PEG with different molecular weight as pore-forming agents: a) borated zirconias, b) tungstophosphoric acid-modified borated zirconias, c) tungstophosphoric acid-modified zirconias.

Table 1
Textural properties of the samples calcined at 320 °C obtained using various pore-forming agents.

Sample	S_{BET}(m^2/g)	S_{micro}(m^2/g)	V_p(cm^3/g)	MPS(nm)
ZrP4	131.5	–	0.10	3.0
ZrP20	166.9	14.3	0.11	3.0
ZrP60	116.5	2.3	0.09	3.1
ZrP4B	214.9	61.1	0.14	3.4
ZrP20B	207.1	62.7	0.13	3.2
ZrP60B	214.0	46.1	0.14	3.3
ZrP4TPA	96.4	–	0.07	3.1
ZrP20TPA	113.9	19.5	0.07	3.0
ZrP60TPA	83.0	2.8	0.06	3.0
ZrP4BTPA	151.6	56.7	0.09	3.3
ZrP20BTPA	147.4	51.2	0.10	3.6
ZrP60BTPA	147.4	48.5	0.10	3.5

PEGs increases the mean pore size and also reduces the presence of microporous. Additionally, higher specific surface area values can be achieved using PEG 2000.

Both, S_{BET} and S_{micro}, of the zirconias obtained by adding PEG during the synthesis and modified with boric acid (ZrP4B, ZrP20B, and ZrP60B samples) are higher than those of the corresponding bare zirconia (Zr sample) (Table 1). Besides, the total pore volume (V_p) and the mean pore size, also increased. This fact may be explained considering that boron species are well dispersed on the surface of the hydrated zirconium oxide and inhibits particle growth during the calcination step, as was reported for diverse oxides supported on zirconia [31].

On the other hand, the textural behaviour of the TPA modified zirconias (ZrP4TPA, ZrP20TPA, and ZrP60TPA samples) was different to that observed for the borated zirconias samples. The specific surface area and the pore volume are lower than those of the corresponding supports, while the mean pore size is not modified. It can be inferred that the tungstophosphate anions ($[PW_{12}O_{40}]^{3-}$) are not as well dispersed as boron species on the surface of the hydrated zirconium oxide, probably due to its higher size (~1.2 nm) and shape (almost spherical). As result they did not inhibits efficiently the zirconia particle growth during the calcination step.

Additionally, as result of the TPA addition to the ZrP4B, ZrP20B, and ZrP60B samples (borated zirconias) both S_{BET} and V_p values of ZrP4BTPA, ZrP20BTPA, and ZrP60BTPA materials decreased, while MPS remains practically unchanged. The lower S_{BET} and V_p values can be due to the a partial pore blockage by the $[PW_{12}O_{40}]^{3-}$ anions. However, these values are still higher than those obtained when zirconia was modified only with TPA.

From the FT-IR spectra, it can be concluded that the washing of the prepared supports appears to be successful, because the several characteristic bands of PEGs, with maxima placed between 529 and 1467 cm^{-1}, being the strongest that attributed to the vibration of the C—O bond located at 1115 cm^{-1} [32], are not observed. However, an undetectable and unimportant amount of the PEGs in the solids could not be dismissed.

The FT-IR spectra of the solids obtained by impregnation of the zirconia with boron, ZrP4B, ZrP20B, and ZrP60B samples, presented a wide band extended between 400 and 1750 cm^{-1} (Fig. 2a), mostly attributed to vibrations of (O—Zr—O) bonds of zirconia between 400 and 1150 cm^{-1} [33]. Some maxima are overlapped to the broad band of zirconia. A band that appeared at 1623 cm^{-1} with a shoulder at 1383 cm^{-1} is ascribed to the bending vibrations of the (H—O—H) and (O—H—O) bonds, respectively. In addition, the characteristic bands of boron species, with the most intense peaks at 881 and 1190 cm^{-1}, are less visible, which may be due to the overlapping.

With regard to the ZrP4TPA, ZrP20TPA and ZrP60TPA samples synthesized by impregnation of the zirconias with TPA, the characteristic bands of bulk TPA are observed, overlapped with the wide band of zirconia (Fig. 2c). The FT-IR spectrum of bulk $H_3PW_{12}O_{40}$ showed bands at 1081, 982, 888, 793, 595, and 524 cm^{-1} (Fig. 2c), assigned to the stretching vibrations of P—O_a, W—O_d, W—O_b—W, W—O_c—W bonds, and to the bending vibration of O_a—P—O_a bond, and they are in agreement with the results reported in the literature for TPA [34]. It must be remembered that the anion of TPA is composed by a central tetrahedral PO_4 group surrounded by twelve WO_6 groups and, in this context, the subscript *a* designates the oxygen that connects the W addenda and the P heteroatom of the heteropolyanion, *b* and *c* denominates the corner and the edge sharing oxygens of the twelve WO_6 octahedra, and *d* is used to name the terminal oxygens. The presence of the P—O_a, W—O_d, W—O_b—W and W—O_c—W stretching vibrations of $[PW_{12}O_{40}]^{3-}$ anion can be clearly observed.

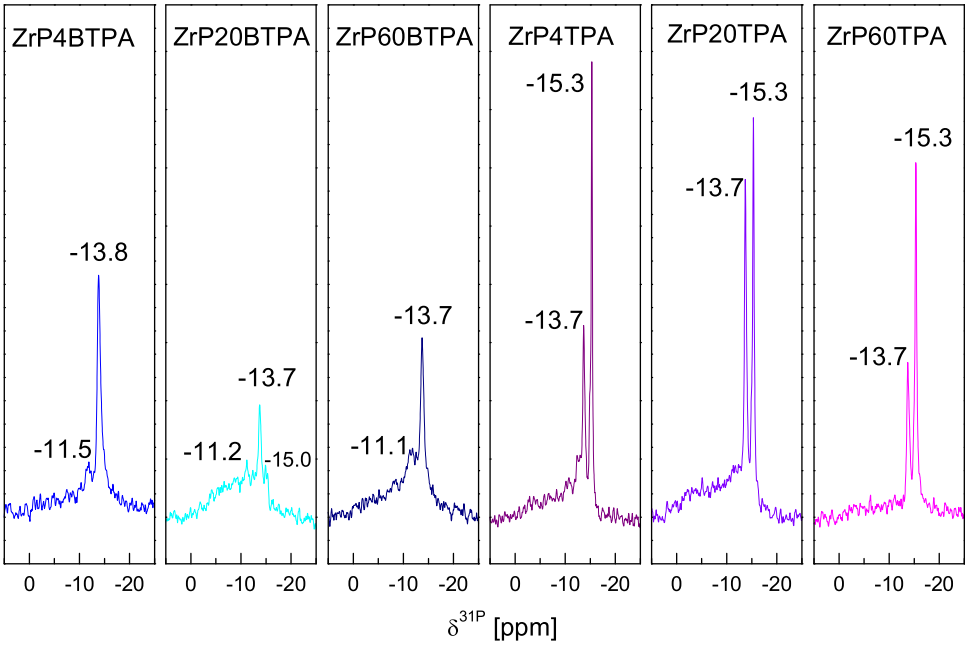

Fig. 3. ^{31}P MAS-NMR spectra of the tungstophosphoric acid-modified borated zirconias and the tungstophosphoric acid-modified zirconias obtained using PEG with different molecular weight as pore-forming agents.

In turn, the FT-IR spectra of the samples prepared by modifying the zirconias with both boron and TPA, ZrP4BTPA, ZrP20BTPA and ZrP60BTPA samples, displayed some special features (Fig. 2b). Actually, the assignment of the observed bands is difficult as they may be attributed to different species. The spectrum of the ZrP20BTPA sample exhibited bands at 1080, 982, 895 and 806 cm^{-1}, together with small bands at 1049 and 961 cm^{-1}. The first two bands can undoubtedly be assigned to the tungstophosphate anion, while the other bands could also be assigned to the lacunar $[PW_{11}O_{39}]^{7-}$ anion, whose main bands are placed at 1100, 1046, 958, 904, 812, and 742 cm^{-1}, though the presence of the $[P_2W_{21}O_{71}]^{6-}$ anion, which displays bands at 1096, 1086, 1030, 983, 967, 933, 882, and 800 cm^{-1} [35], cannot be discarded.

With regard to the ZrP4BTPA and ZrP60BTPA samples, whose spectra present bands with maxima at 1056, 961, 896 and 824 cm^{-1}, and a shoulder at 1085 cm^{-1}, the presence of the lacunar $[PW_{11}O_{39}]^{7-}$ anion can be inferred; however, the widening of the bands may be a result of the overlapping with the bands of the $[P_2W_{21}O_{71}]^{6-}$ anion. It must be borne in mind that the tungstophosphate anion can undergo a transformation, following the scheme proposed by Pope [36], that is $[PW_{12}O_{40}]^{3-} \Leftrightarrow [P_2W_{21}O_{71}]^{6-} \Leftrightarrow [PW_{11}O_{39}]^{7-}$, attributed to the limited stability range of the $[PW_{12}O_{40}]^{3-}$ anion with a pH increase.

The ^{31}P MAS-NMR spectra of the samples containing tungsten are shown in Fig. 3. For the samples obtained by impregnating the zirconias with TPA, ZrP4TPA, ZrP20TPA and ZrP60TPA samples, the main line is placed at −15.3 ppm, assigned to the $[PW_{12}O_{40}]^{3-}$ anion, accompanied by a line at −13.7 ppm, which can be attributed to the $[P_2W_{21}O_{71}]^{6-}$ dimeric species [37]. Nevertheless, the line assigned to the $[PW_{12}O_{40}]^{3-}$ anion is the most intense in all the samples, while the ratio between the intensity of the line placed at −15.3 ppm and that of the band at −13.7 ppm decreased in the order ZrP4TPA > ZrP60TPA > ZrP20TPA. The results are in agreement with those obtained by FT-IR, although the presence of the $[P_2W_{21}O_{71}]^{6-}$ species could not be entirely confirmed by FT-IR.

On the other hand, the ^{31}P MAS-NMR spectra of the samples prepared by impregnation with both boron and TPA (ZrP4BTPA, ZrP20BTPA and ZrP60BTPA samples) presented lines at −13.7 ppm and a signal at −11.2 ppm, which may be assigned to the $[P_2W_{21}O_{71}]^{6-}$ and $[PW_{11}O_{39}]^{7-}$ anion, respectively. The ZrP20BTPA sample presented, in addition, a weak signal assigned to the tungstophosphate anion at −15.0 ppm. The results are in agreement with those obtained by FT-IR.

In brief, the physicochemical characterization of the samples containing TPA indicated that the tungstophosphate anion remains unchanged when it interacts directly with the prepared zirconias during impregnation, while it partially or totally changes when interacting with borated zirconias.

The SEM micrographs of all the samples depicted in Fig. 4 illustrated that inhomogeneous-sized particles are present. The zirconias impregnated with boron (ZrP4B, ZrP20B, and ZrP60 B samples) showed a rather compact structure, which is almost maintained when they are also impregnated with TPA (ZrP4BTPA, ZrP20BTPA and ZrP60BTPA samples). Regarding the samples obtained by only impregnating TPA on zirconia (ZrP4TPA, ZrP20TPA and ZrP60TPA samples), some small TPA crystallites can be perceived on the support surface, though TPA addition barely changed the structure of the parent support. The micrographs give some evidence that, in most of the samples, a rather spongy structure is obtained when PEG2000 is employed as pore-forming agent, though the samples presented a closer structure when using PEG 400 or PEG6000.

It must be pointed out that the polymer PEG400 have short helices and, added during the samples preparation, can aid to obtain materials with somewhat tight structure. By contrast, it was reported that, for PEG2000, the PEG chains in the sol form micelles, and the oxide particles enclose them, so aggregate type morphology is achieved [38], which would be the cause of the slightly more spongy solids. In the case of PEG6000, it was suggested that PEG chains in the sol tend to assemble in a network structure, which may be attributed to interaction of the (-CH_2CH_2O-) groups of PEG with hydroxyls of the hydrated zirconia, leading to a rather compact morphology.

The samples were titrated with *n*-butylamine, method that allows one to make a comparison of the strength of the acid sites which the solids contain, being the initial electrode potential (Ei) an indication of the maximum strength of the sites. The following scale is recommended to classify the acid sites strength, Ei > 100 mV (very

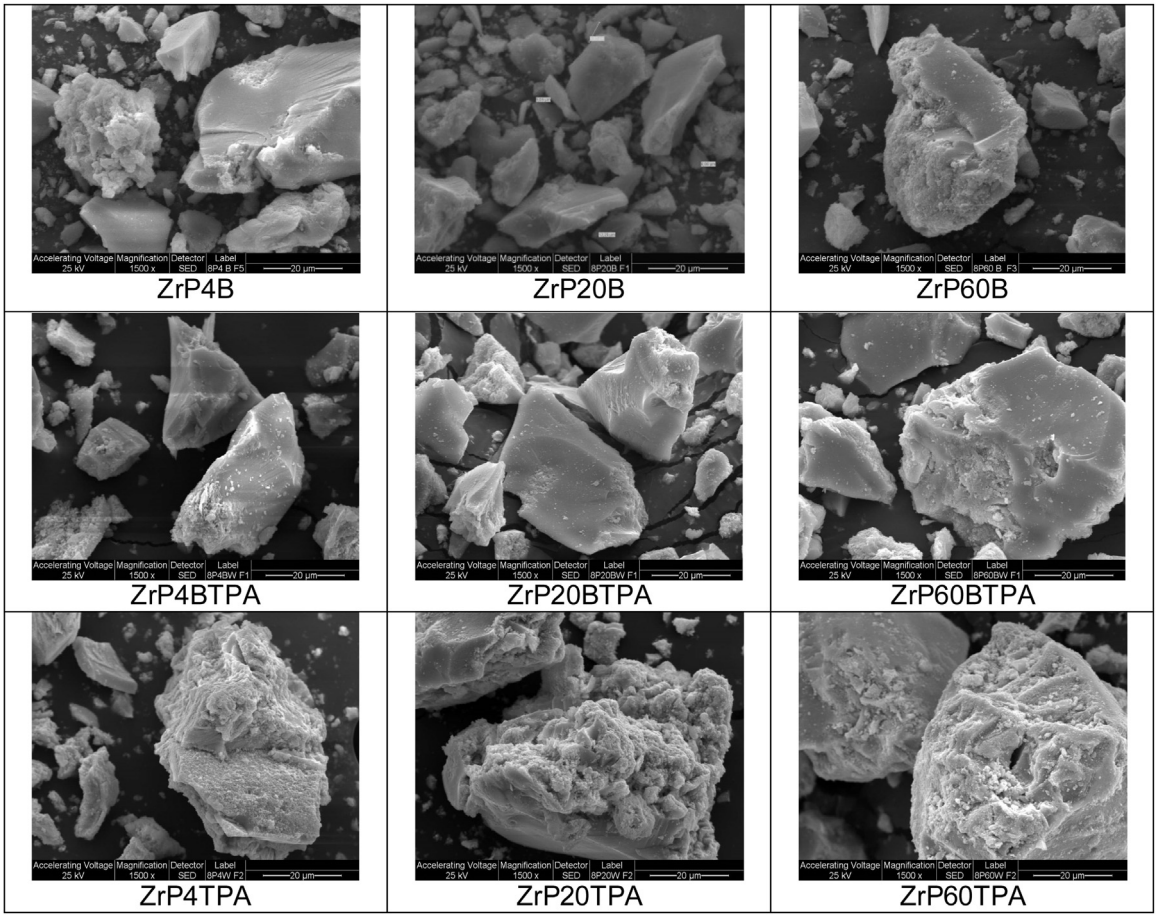

Fig. 4. SEM micrographs of the samples obtained using different pore-forming agents. Magnification: 1500×. Bar: 20 μm.

strong sites), 0 < Ei < 100 mV (strong sites), −100 < Ei < 0 mV (weak sites) and Ei < −100 mV (very weak sites),.

All the borated zirconias exhibited very strong acid sites (Fig. 5a), which would be a consequence of the boron species well dispersed on the surface of the hydrated zirconia, as observed by XRD. This can promote the acidity of the materials due to Lewis acid sites of the zirconium atoms can be enhanced by an inductive effect and Brønsted acid sites can be produced by hydration of the boron species [40]. The obtained Ei values were 152, 184 and 205 mV for the ZrP4B, ZrP20B, and ZrP60B samples, respectively. The lower Ei value of the sample obtained by impregnation of boron solution on zirconia prepared using PEG400 may be related to the somewhat more closed morphology of this material.

The samples containing TPA presented higher acidity than the borated zirconias. The ZrP4TPA, ZrP20TPA and ZrP60TPA samples presented Ei values of 336, 311 and 309 mV, respectively, and the values corresponding to the ZrP4BTPA, ZrP20BTPA and ZrP60BTPA samples were 295, 228 and 227 mV, respectively. This may be due to the high acidic characteristics of the Keggin heteropolycompounds.

3.2. Catalytic tests

The catalytic properties of the prepared samples were studied in the esterification reaction of 2-phenylethanol with acetic acid (Scheme 1).

The catalytic behavior of all the synthesized materials, namely zirconias obtained using PEG of different molecular weight as pore-forming agents and impregnated with boric acid and/or TPA (ZrP4B, ZrP20B, ZrP60B; ZrP4TPA ZrP20TPA, ZrP60TPA; ZrP4BTPA, ZrP20BTPA, and ZrP60BTPA samples), was compared. In all the tests, the reaction conditions employed were selected based on previous results of our research group [9,10], and the values are those indicated in Experimental.

Fig. 6 shows the results, expressed as 2-phenylethanol conversion, obtained in the esterification reaction of 2-phenylethanol with acetic acid using zirconia modified with boric acid (ZrP4B, ZrP20B, and ZrP60 B samples) as catalysts. Though at short times the ZrP20 B sample gave a lower conversion, it led to a slightly higher value from 7 h onwards; the similarity may be related to almost the same physicochemical characteristics of the samples prepared with the zirconias obtained using PEG of different molecular weight.

On the other hand, Fig. 7 shows the data obtained on the esterification reaction of 2-phenylethanol with acetic acid using as catalysts the zirconias modified by impregnation with a TPA solution (ZrP4TPA, ZrP20TPA, and ZrP60TPA samples), expressed as 2-phenylethanol conversion. The conversions attained were higher than those corresponding to the zirconias doped only with boron. This fact is directly related to the higher acid strength of these catalysts. The ZrP4TPA sample exhibited the highest conversion; at 7 h the conversion was 96% and significantly rose up to 99% after 14 h, without the presence of by-products. Evidently, the behavior of the ZrP4TPA catalyst is in accordance with the fact that this sample is the most acidic material.

The results of the conversion evolution in the esterification reaction of 2-phenylethanol with acetic acid catalyzed by borated zirconias modified with TPA (ZrP4BTPA, ZrP20BTPA, and ZrP60BTPA samples) are presented in Fig. 8. Within this group of catalysts, the ZrP20BTPA sample gave the highest conversion (58% at a reaction time of 7 h), with an excellent selectivity. Nevertheless, the conversion results obtained were lower than those of the

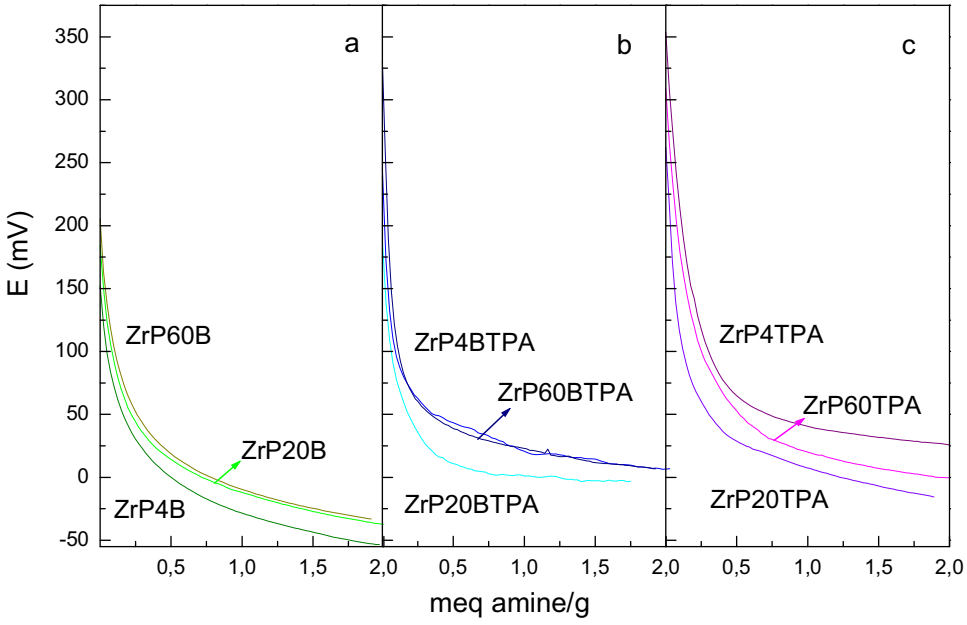

Fig. 5. Potentiometric titration curves of the samples obtained using PEG with different molecular weight as pore-forming agents: a) borated zirconias, b) tungstophosphoric acid-modified borated zirconias, c) tungstophosphoric acid-modified zirconias.

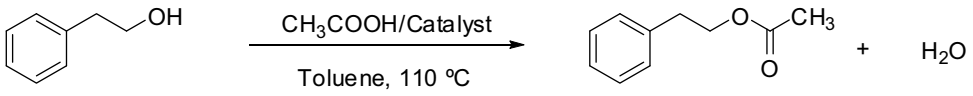

Scheme 1. Esterification of 2-phenylethanol with acetic acid.

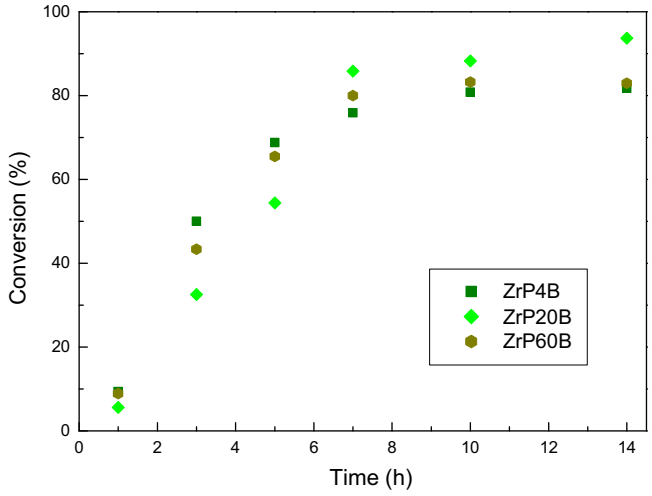

Fig. 6. Conversion obtained with boric acid-modified zirconias as catalysts in the 2-phenylethanol esterification with acetic acid.

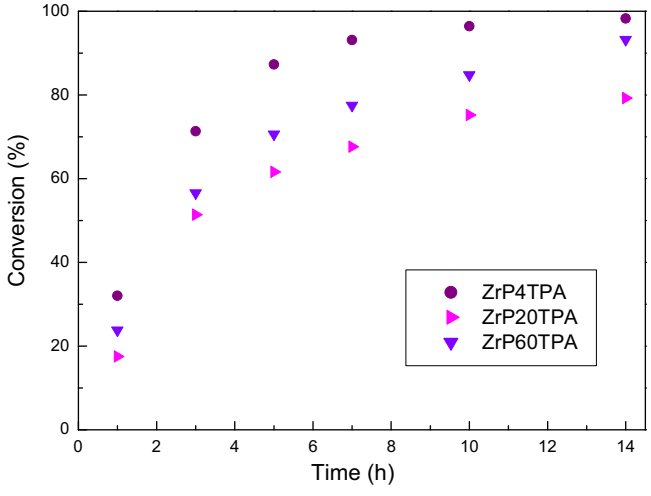

Fig. 7. Conversion obtained with TPA-modified zirconias as catalysts in the 2-phenylethanol esterification with acetic acid.

other two families of catalysts when the zirconias were doped with both boric acid and TPA. This fact must be related to the total or partial change of the tungstophosphate anion into other species, as observed from FT-IR and ^{31}P MAS-NMR. It can be noted that, within this group of materials, the ZrP20BTPA sample, which led to the highest conversion, is the only solid that showed the presence of the undegraded tungstophosphate anion by both techniques.

The catalyst that exhibited the best performance (ZrP4TPA sample) was used to carry out a preparative synthesis of 2-phenylethyl acetate, an essential aroma component for the food and cosmetic industries. Excellent selectivity and yield to pure ester (98%) were obtained carrying out the reaction at 110 °C using this most active catalyst. The reusability of the catalyst was checked after the catalyst separation from the reaction mixture, washing, and drying prior to its reuse. However, when the catalyst was reused, a high yield decrease was observed, which could be attributed to a TPA leaching from the solid. So, the borated zirconia that gave the best conversion (ZrP20 B sample) was chosen to be employed as catalyst, thus obtaining a yield to the pure ester of 96% with excellent selectivity, as no by-product was observed, similarly to all the reactions carried out. The reuse of this material in the reaction, following the previous detailed procedure, was performed and, in this case, no significant loss in the product yield was observed, the

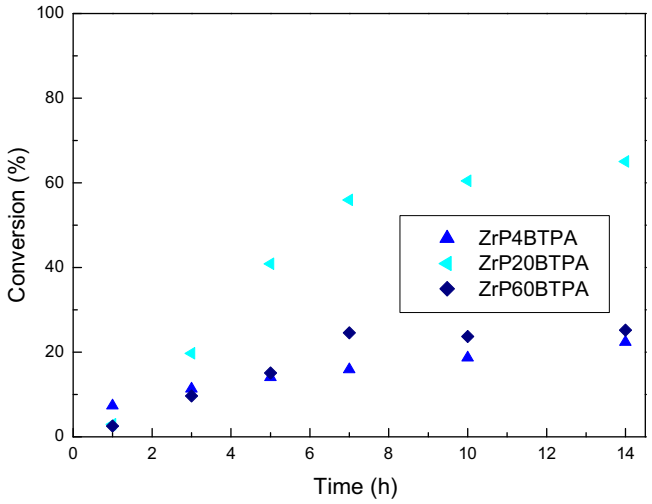

Fig. 8. Conversion obtained with zirconias modified with both boric acid and TPA as catalysts in the 2-phenylethanol esterification with acetic acid.

Table 2
Acetylation of 2-phenylethanol with acetic acid. Yields obtained using different catalysts.

Entry	Catalyst	Time (h)	Yield (%)	Reference
1	ZrP4TPA	14	96	This work
2	$Sc(OTf)_3$	24	99	Barret [38]
3	$K_5CoW_{12}O_{40}{\cdot}3H_2O$	1	98	Habibi [39]
4	$Cp_2Ti(OSO_2C_8F_{17})_2$	2	99	Qiu [40]
5	Borated zirconia with ammonium metatungstate	14	83	Osiglio [10]
6	$Yb(CNf_3)_3$	18	60	Barret [41]

yield obtained being 95% and 94% for the second and third cycles, respectively.

The yields obtained in this work using ZrP4TPA (Table 2, entry 1) are comparable to those obtained by Barret, Habibi and Qiu (Table 2, entries 2–4), slightly higher than those reported previously by our group (Table 2, entry 5), and clearly superior to those achieved by Barret in 2003 (Table 2 entry 6)

Then this solid was probed as catalyst in the esterification of different alcohols and phenols with acetic acid, under the same experimental conditions, and the results of yield to esters attained are listed in Table 3.

As a relationship between the sulfide oxidation easiness and the sulfur atom charge obtained by a computational method was recently found by our research group, and the result was associated with the nucleophilicity of the sulfur atom in the sulphide substrate [41], in the present paper a correlation between the oxygen nucleophilicity and the reactivity of the different tested alcohols and phenols was intended, using a semi-empirical method. The relationship between the electronic density (De) of the oxygen atoms, which was estimated by Hyperchem release 5, and the reaction yield to acetylated alcohols and phenols was analyzed. The electronic density on the oxygen atom of all the studied alcohols and phenols, which varied between −0.330 and −0.237, is also presented in Table 3. From the results obtained, it could be observed that alcohols (De = −0.330 to −0.326) are more reactive than phenols (De = −0.253 to −0.237). The different reactivity between these two groups is associated with the electronic density on the oxygen, since a higher electronic density on this atom helps in the nucleophilic attack on the electrophilic carboxylic carbon in the acetic acid. In the case of phenols, the diminution of electronic density is due to an electronic delocalization by resonance in the benzene ring.

The reactivity difference between the diverse tested alcohols cannot be explained by an electronic effect. This trend is reasonable since in all the studied alcohols the charge on the oxygen atom (calculate by Hyperchem), which determines its nucleophilicity, was very similar. The steric component affecting the alcohol reactivity is also a decisive factor for Fischer acid-catalyzed esterification [9]. The steric hindrance increases with molecular size, inducing electronic repulsion between nonbonded atoms of the reacting molecules [42]. The reactivity of 2-phenylethanol, 2-phenoxyethanol, and 1-hexanol (primary alcohols) and 4-methylbenzyl alcohol (benzylic alcohol) (Table 3, entries 1–4, yield: 95%-85%) was higher than that of 1-cyclohexanol (secondary alcohol) (Table 3, entry 5, yield: 65%)

The yield difference between primary and secondary alcohols can be attributed to steric effects that considerably affect the acetylation rate. The presence of bulky groups, not far from the reaction center, either in the alcohol or in the acid, slows down the esterification rate, as the most sterically hindered alcohols give a lower yield. Similarly, for the very bulky *t*-butanol (a tertiary alcohol) no reaction was detected under similar reaction conditions (Table 3, entry 6).

On the other hand, the yield of phenol acetylation was lower than that of the primary and secondary alcohols, reaching only values of 13% to 20% for different phenols (Table 3, entries 7–9). The atomic charge on the oxygen atom was −0.253, −0.253, and −0.248 for phenol, 4-methyl phenol and 4-chloro phenol, respectively. In these cases, there is a relationship between the oxygen atom charge and the reaction yield. The 4-nitrophenol (atomic charge on the oxygen atom: −0.237), a phenol with a strong electron-withdrawing group, fails to give the expected acetylation product (Table 3, entry 10).

In sum, the reactivity order towards acetylation with acetic acid using the studied catalyst was as follows: primary alcohols > secondary alcohols > phenols.

4. Conclusions

Zirconias prepared with polyethylene glycol of different molecular weight as pore-forming agents modified with boron or tungstophosphoric acid were very efficient and selective catalysts for the esterification of 2-phenylethanol with acetic acid, while samples impregnated with both boric acid and tungstophosphoric acid gave low yields. The behavior of the latter samples is due to the total or partial change of the tungstophosphate anion into other species. The catalyst obtained by impregnating tungstophosphoric acid on zirconia prepared using a 400 Da polyethylene glycol as pore-forming agent exhibited the best yield to pure ester (98%) with excellent selectivity (100%), though it did not perform well during its reuse due to TPA leaching. However, the catalyst obtained by impregnation of boric acid on zirconia prepared using a 2000 Da polyethylene glycol allowed overcoming this difficulty and could be reused without a significant yield decrease.

The electronic density on the oxygen atom of all the studied alcohols (De = −0.330 to −0.326) and phenols (De = −0.253 to −0.237), was estimated by Hyperchem release 5. The difference in reactivity between alcohols and phenols in their esterification with acetic acid was correlated with the electronic density of the oxygen atom. A higher electronic density on this atom makes easier in the nucleophilic attack on the electrophilic carboxylic carbon in the acetic acid.

The reactivity difference between the primary, secondary and tertiary tested alcohols cannot be explained by an electronic effect since in all the studied alcohols the charge on the oxygen atom, was very similar. In this case, the difference can be attributed to steric effects that considerably affect the reactivity.

Table 3
Yield to esters and electronic density of the substrates.

Entry	Substrate	Product	Yield (%)	De
1	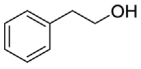	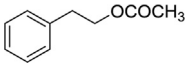	96 (95, 94)	−0.330
2	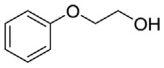	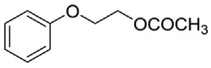	88	−0.329
3	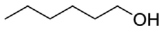	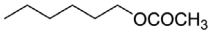	95	−0.329
4	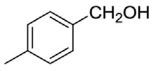	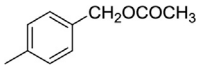	85	−0.326
5		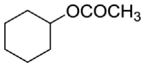	65	−0.328
6		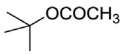	–	−0.326
7		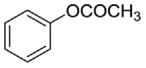	20	−0.253
8	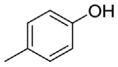	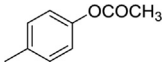	19	−0.253
9	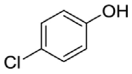	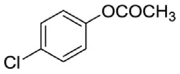	13	−0.248
10	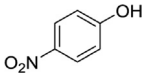	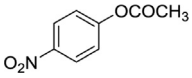	–	−0.237

De = Atomic charge calculated by Hyperchem 5.0.

The use of this type of solid catalyst and acetic acid as acylating agent is a green alternative to the classical procedures, because they lead to a cheap and clean process, only giving water as by-product.

Acknowledgements

The authors thank G. Valle, M. Theiller and E. Soto for their experimental contribution, and UNLP (X638) and CONICET (PIP 628) for the financial support.

References

[1] T.W. Green, P.J.M. Wuts, Protective Groups in Organic Synthesis, Wiley, New York, 1999.
[2] P. Kumar, R. Pandey, M. Bodas, S. Dagade, M. Dongare, A. Ramaswamy, J. Mol. Catal. A: Chem. 181 (2002) 207–213.
[3] T. Reddy, M. Narasimhulu, N. Suryakiran, Ch. Mahesh, K. Ashalatha, Y. Venkateswarlu, Tetrahedron Lett. 47 (2006) 6825–6829.
[4] M.A. Longo, M.A. Sanromán, Food Technol. Biotechnol. 44 (2006) 335–353.
[5] L. Rajabi, R. Luque, Catal. Commun. 45 (2014) 129–132.
[6] E. Albertazzi, R. Cardillo, S. Servi, G. Zuchi, Biotechnol. Lett. 16 (1994) 491–496.
[7] H. Yan, Q. Zhang, Z. Wang, Catal. Commun. 45 (2014) 59–62.
[8] F. Shirini, M. Zolfigol, K. Mohammadi, Bull. Korean Chem. Soc. 25 (2004) 325–327.
[9] L. Osiglio, G. Romanelli, M. Blanco, J. Mol. Catal. A: Chem. 316 (2010) 52–58.
[10] L. Osiglio, A. Sathicq, G. Romanelli, M. Blanco, J. Mol. Catal. A: Chem. 359 (2012) 97–103.
[11] L.R. Pizzio, C.V. Cáceres, M.N. Blanco, Appl. Catal. A: Gen. 167 (1998) 283–294.
[12] M.E. Chimienti, L.R. Pizzio, C.V. Cáceres, M.N. Blanco, Appl. Catal. A: Gen. 208 (2001) 7–19.
[13] V.D. Monopoli, L.R. Pizzio, M.N. Blanco, Mater. Chem. Phys. 108 (2008) 331–336.
[14] M.N. Blanco, L.R. Pizzio, Appl. Surf. Sci. 256 (2010) 3546–3553.
[15] D.P. Sawant, A. Vinu, Josena Justus, P. Srinivasu, S.B. Halligudi, J. Mol. Catal. A: Gen. 276 (2007) 150–157.
[16] D.P. Sawant, J. Justus, V.V. Balasubramanian, K. Ariga, P. Srinivasu, S. Velmathi, S.B. Halligudi, A. Vinu, Chem. Eur. J. 14 (2008) 3012–3200.
[17] B.M. Devassy, S.B. Halligudi, S.G. Hegde, A.B. Halgeri, F. Lefebvre, Chem. Commun. (2002) 1074–1075.
[18] E. Rafiee, N. Nobakht, J. Mol. Catal. A: Chem. 398 (2015) 17–25.
[19] A. Patel, N. Narkhede, S. Singh, S. Pathan, Catal. Rev. 58 (2016) 337–370.
[20] M. Gorsd, G. Sathicq, G. Romanelli, L. Pizzio, M. Blanco, J. Mol. Catal. A: Chem. 420 (2016) 294–302.
[21] L. Pizzio, C. Cáceres, M. Blanco, Appl. Surf. Sci. 151 (1999) 91–101.
[22] L.R. Pizzio, M.N. Blanco, Appl. Catal. A: Gen. 255 (2003) 265–277.
[23] L. Hu, Y. Sun, L. Lin, S. Liu, Biomass Bioenergy 47 (2012) 289–294.
[24] Y. Wei, D. Jin, T. Ding, W. Shih, X. Liu, S. Cheng, Q. Fu, Adv. Mater. 10 (1998) 313–316.
[25] J. Zheng, J. Pang, K. Qiu, Y. Wei, Microporous Mesoporous Mater. 49 (2001) 189–195.
[26] L. Pizzio, Mater. Lett. 59 (2005) 994–997.
[27] L. Osiglio, M. Blanco, Procedia Mater. Sci. 1 (2012) 491–498.
[28] B.L. Kirsch, S.H. Tolbert, Adv. Funct. Mater. 13 (2003) 281–288.
[29] J.C. Duchet, M.J. Tilliette, D. Cornet, Catal. Today 10 (1991) 507–520.
[30] T. Yamaguchi, Catal. Today 20 (1994) 199–217.
[31] B. Zhao, X. Xu, H. Ma, D. Sun, J. Gao, Catal. Lett. 45 (1997) 237–244.
[32] D. Zuo, Y. Xu, W. Xu, H. Zou, Chin. J. Polym. Sci. 26 (2008) 405–414.
[33] S. Vives, C. Guizard, L. Cot, C. Oberlin, J. Mater. Sci. 34 (1999) 3127–3135.
[34] C. Rocchiccioli-Deltcheff, R. Thouvenot, R. Franck, Spectrochim. Acta 32A (1976) 587–597.
[35] A.V. Ivanov, T.V. Vasina, V.D. Nissenbaum, L.M. Kustov, M.N. Timofeeva, J.I. Houzvicka, Appl. Catal. A: Gen. 259 (2004) 65–72.
[36] M.T. Pope, Heteropoly and Isopoly Oxometalates, Springer-Verlag, Heidelberg, 1983, pp. 58.
[37] R. Massart, R. Contant, J. Fruchart, J. Ciabrini, M. Fournier, Inorg. Chem. 16 (1977) 2916–2921.
[38] Y. Sun, Y. Wang, W. Guo, T. Wang, G. Luo, Microporous Mesoporous Mater. 88 (2006) 31–37.
[39] Candelaria Leal Marchena, Silvina Gomez, Clara Saux, Liliana B. Pierella, Luis R. Pizzio, Quim. Nova 38 (2015) 518–525.
[40] D. Ravindra, Y. Nie, S. Jaenicke, G. Chuah, Catal. Today 96 (2004) 147–153.
[41] Romina Frenzel, Ángel G. Sathicq, Mirta N. Blanco, Gustavo P. Romanelli, Luis R. Pizzio, J. Mol. Catal. A: Chem. 403 (2015) 27–36.
[42] Y. Liu, E. Lotero, J.G. Goodwin Jr., J. Catal. 243 (2006) 221–228.